

# Evidence of radiation-driven Landau states in 2D electron systems: magnetoresistance oscillations phase shift

JESÚS IÑARREA<sup>1,2</sup>

<sup>1</sup>*Escuela Politécnica Superior, Universidad Carlos III, Leganes, Madrid, Spain* and <sup>2</sup>*Unidad Asociada al Instituto de Ciencia de Materiales, CSIC, Cantoblanco, Madrid, 28049, Spain.*

PACS **nn.mm.xx** – First pacs description  
PACS **nn.mm.xx** – Second pacs description  
PACS **nn.mm.xx** – Third pacs description

**Abstract** –We provide the ultimate explanation of one of the core features of microwave-induced magnetoresistance oscillations in high mobility two dimensional electron systems: the 1/4-cycle phase shift of minima. We start with the radiation-driven electron orbits model with the novel concept of scattering flight-time between Landau states. We calculate the extrema and nodes positions obtaining an exact coincidence with the experimental ones. The main finding is that the physical origin of the phase shift is a delay of  $\frac{\pi}{2}$  of the radiation-driven Landau guiding center with respect to radiation, demonstrating the oscillating nature of the irradiated Landau states. We analyze the dependence of this minima on radiation frequency and power and its possible shift with the quality of the sample.

**Introduction.** – Microwave-induced magnetoresistance ( $R_{xx}$ ) oscillations (MIRO) [1,2], show up in high mobility two-dimensional electron systems (2DES) when they are irradiated with microwaves (MW) at low temperature ( $T \sim 1K$ ) and under low magnetic fields ( $B$ ) perpendicular to the 2DES. At high enough MW power ( $P$ ) maxima and minima oscillations increase but the latter evolve into zero resistance states (ZRS) [1, 2]. Both effects were totally unexpected when they were first obtained revealing some type of new radiation-matter interaction or coupling assisting electron magnetotransport [3–5]. Despite that over the last few years important experimental [6–25] and theoretical efforts [26–42] have been made on MIRO and ZRS, their physical origin still remains controversial and far from reaching a definite consensus among the people devoted to this field. For instance, the two, in principle, accepted theoretical models explaining MIRO, (displacement [31] and inelastic [35] models) are under question in regards of recent (and even older) experimental results [43, 44] that they are not able to explain. In fact, experimentalists on MIRO are calling for other theoretical approaches that might be more successful offering solid arguments on MIRO and ZRS physical origin [26, 27, 32].

Among the different features defining MIRO we can underline some that can be consider as fundamental, turning up in most experiments irrespective of the semicon-

ductor platform and carrier (holes or electrons). Thus, we can highlight three of them: MIRO are periodic in  $B^{-1}$ , MIRO dependence with  $P$  follows a sublinear law whose exponent is around 0.5 [22, 24] and finally they present a 1/4-cycle phase shift in the minima position [8, 11, 45]. To date, none of the existing theoretical models on MIRO have been able to provide a convincing explanation about the minima shift and why they depends in such a way on MW frequency ( $w$ ) and  $B$  or cyclotron frequency ( $w_c$ ). On the other hand they are, according to experiments, immune to MW power.

In this letter, we present, based on the radiation-driven electron orbits model [26–28], a theoretical analysis on MIRO where we explain the 1/4-cycle shift of minima and the peculiar position of the extrema and nodes. According to this model, when a Hall bar is illuminated, the guiding centers of the Landau states perform a classical trajectory consisting in a harmonic motion along the direction of the current. Thus, the electron orbits move in phase and harmonically with each other at the radiation frequency, altering dramatically the scattering conditions and giving rise eventually to MIRO and, at higher  $P$ , ZRS. Now, our approach consists on two main physical effects. The first is that the Landau orbit guiding center displacement lags behind the driving force (radiation) by a definite phase constant of  $\frac{\pi}{2}$ . And secondly, in a scenario of remote

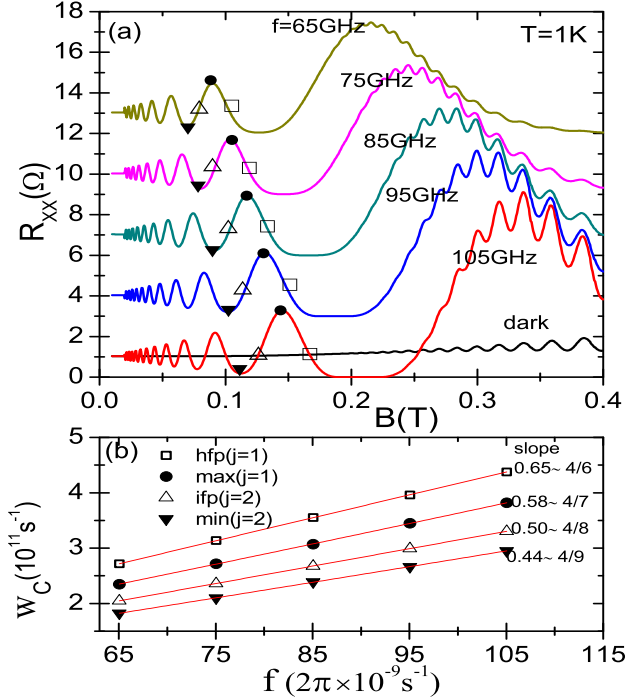


Fig. 1: Dependence of MIRO extrema and nodes with radiation frequency. 1a) Calculated  $R_{xx}$  versus  $B$  under radiation for several frequencies (from 65 GHz to 105 GHz). The dark curve is also presented. Extrema and nodes displace to higher  $B$  as  $w$  increases. 1b) Cyclotron frequency  $w_c$  vs radiation frequency  $w = 2\pi f$ , where  $f$  is the frequency in GHz, for the extrema and nodes labelled in the upper panel. For the hfp, the square symbol, for the maxima, the black dot symbol, for the ifp, the triangle symbol and finally, for the minima, black down triangle. In panel we plot also the fits of the four sets of data giving straight lines. The slopes correspond with the extrema and nodes positions of the upper panel.

charged impurity scattering, we introduced the concept of scattering *flight time* as the time it takes the electron to jump from one Landau orbit to another in a scattering process. The core finding is that this time is equal to the cyclotron period. Thus, during the flight time the electrons complete one loop in their cyclotron orbits. For the second effect to happen it is essential that magnetotransport is dominated by the guiding center position of the Landau orbit.

In our calculations we recover the experimental expressions for the extrema and nodes positions showing that only depend on  $w$  and  $w_c$ . We finally discuss and predict the situation of a possible change in the minima shift for ultrahigh mobility samples when ramping up the magnetic field. The reason is that the phase constant delay of the MW-driven guiding center with respect to radiation, depends on the damping that the Landau orbits suffer along the swinging motion. This damping drops in samples with extreme high mobility (much lower disorder), affecting the

phase constant (delay) and eventually the extrema positions and minima shift.

**Theoretical Model.** – The *radiation-driven electron orbits model*, was proposed to study the magnetoresistance of a 2DES subjected to MW at low  $B$  and temperature,  $T$  [26, 27, 46–48]. The total electronic hamiltonian  $H$  can be exactly solved and the solution for the total wave function of  $H$  [26, 36, 46–48] reads:  $\Psi_n(x, t) \propto \phi_n(x - X_0 - x_{cl}(t), t)$ , where  $\phi_n$  is the solution for the Schrödinger equation of the unforced quantum harmonic oscillator. Thus, the obtained wave function (Landau state or Landau orbit) is the same as the one of the standard quantum harmonic oscillator where the guiding center of the Landau state,  $X_0$  without radiation, is displaced by  $x_{cl}(t)$ .  $x_{cl}(t)$  is the classical solution of a negatively charged, forced and damped, harmonic oscillator [49, 50]:

$$\begin{aligned} x_{cl}(t) &= \frac{-eE_0}{m^* \sqrt{(w_c^2 - w^2)^2 + \gamma^4}} \cos(wt - \beta) \\ &= -A \cos(wt - \beta) \end{aligned} \quad (1)$$

where  $E_0$  is the amplitude of the MW electric field and  $\beta$  is a phase constant.  $\beta$  is the phase difference between the radiation-driven guiding center and the driving radiation; its expression reads,  $\tan \beta = \frac{\gamma^2}{w_c^2 - w^2}$ . Thus, the guiding center lags behind the time-dependent driving force, (radiation), a phase constant of  $\beta$ . In the above calculations radiation has been expressed as  $E(t) = E_0 \cos wt$ .  $\gamma$  is a phenomenologically-introduced damping factor for the interaction of electrons with the lattice ions giving rise to the emission of acoustic phonons. When the damping parameter  $\gamma$  is important, ( $\gamma > w \Rightarrow \gamma^2 \gg w^2$ ), then  $\tan \beta \rightarrow \infty$  and  $\beta \rightarrow \frac{\pi}{2}$ . Now, the time-dependent guiding center is,  $X(t) = X_0 + x_{cl}(t) = X_0 - A \sin wt$ . This physically implies that the orbit guiding centers oscillate harmonically at the MW frequency, but radiation leads the guiding center displacement in  $\frac{\pi}{2}$ . This expression automatically fulfills the initial condition of  $X(t = 0) = X_0$  and then we do not need to add any initial phase.

This *radiation – driven* behavior of the orbit guiding centers is supposed to affect the electron-charged impurity scattering and eventually  $R_{xx}$  [47, 51, 52]. If one electron, without radiation, is scattered from the Landau state  $\Psi_n$  located at  $X_{0,n}$  to the final state  $\Psi_m$  at  $X_{0,m}$  in a time  $\tau$ , the average advanced distance, is given by  $\Delta X_0 = X_{0,m} - X_{0,n}$ . This *flight time*,  $\tau$ , is the time it takes the electron to “fly” from one orbit to another due to scattering. This time is part of the quantum scattering time, (quantum lifetime),  $\tau_q$ , that it is normally defined as the average time between scattering events or collisions, considering that all of them are equally weighted. In high mobility 2DES the electron magnetotransport is ruled or dominated by the guiding center position of the Landau orbit and not by the electron position itself. In a semiclassical approach, this implies that the electron scattering begins and ends in the same relative position inside the

initial and final cyclotron orbits. In other words, during the scattering jump from one orbit to another, in a time  $\tau$ , the electrons in their orbits complete one full loop. Then,  $\tau$  must be equal to  $T_c$ :  $\tau = \frac{2\pi}{w_c} = T_c$  where  $T_c$  is the cyclotron period. Interestingly, applying the time-energy uncertainty relation [53]  $\Delta t \cdot \Delta E \geq \hbar$ , it turns out that, being  $\Delta t = \tau$ , then,  $\tau \times \Delta E = \frac{2\pi}{w_c} \times \Delta E \geq \hbar \Rightarrow$  the uncertainty of energy is,  $\Delta E \simeq \hbar w_c$ . Then the scattered electron ends up, most likely, in the next Landau level:  $m = n + 1$ .

When we turn on radiation, the guiding centers begin to harmonically oscillate according to the expression of  $X(t)$ . Later, in a time  $t_i$ , scattering starts and the electron jumps from  $\Psi_n(t)$  at  $X_n(t)$  to  $\Psi_m(t)$  at  $X_m(t)$  in a total time  $t_f = t_i + \tau$ . The average advanced distance will change accordingly:  $\Delta X(t) = X_m(t_f) - X_n(t_i) = \Delta X_0 - A \sin w(t_i + \tau) + A \sin w t_i$ . The time  $t_i$  is on average the time it takes the electron to experience a scattering proces, i.e., the scattering time  $\tau_q$ , that for constant  $B$  it is constant too. Therefore,  $t_i \simeq \tau_q$  and  $\Delta X(t) = \Delta X_0 - A \sin(\tau + \phi) + A \sin \phi$ , being  $\phi = w\tau_q$ . Now shifting the time origin so that  $\phi = 0$ , i.e., to when the electron scattering begins, we obtain the final expression:  $\Delta X(t) = \Delta X_0 - A \sin w\tau$ .

The longitudinal conductivity  $\sigma_{xx}$  is given by [54]  $\sigma_{xx} \propto \int dE \frac{(\Delta X^{MW})^2}{\tau_q}$  being  $E$  the energy and  $\frac{1}{\tau_q}$  is the remote charged impurity scattering rate [26]. To obtain  $R_{xx}$  we use the common tensorial relation  $R_{xx} = \frac{\sigma_{xx}}{\sigma_{xx}^2 + \sigma_{xy}^2} \simeq \frac{\sigma_{xx}}{\sigma_{xy}^2}$ , where  $\sigma_{xy} \simeq \frac{n_i e}{B}$ ,  $n_i$  being the electrons density, and  $\sigma_{xx} \ll \sigma_{xy}$ . Thus [52],  $R_{xx} \propto -A \sin w\tau$ .

Importantly, according to the last expression, the MIRO minima positions are given by:  $w\tau = \frac{\pi}{2} + 2\pi j \Rightarrow w = \frac{2\pi}{\tau} (\frac{1}{4} + j)$ ,  $j$  being a positive integer. And for the MIRO maxima:  $w\tau = \frac{3\pi}{2} + 2\pi j \Rightarrow w = \frac{2\pi}{\tau} (\frac{3}{4} + j)$ . We can obtain also expressions for MIRO nodes, or the points where the radiation curve crosses the dark curve. The right nodes, also known as *half integer fixed points* (hifp), fulfill,  $w = \frac{2\pi}{\tau} (j + 1/2)$ . And the left ones, known as *integer fixed points* (ifp),  $w = \frac{2\pi}{\tau} j$ . If we compare the calculated expression with the ones previously obtained in experiments by Mani et al [8,11]:

theory	$\Longleftrightarrow$	experiment	
$min \rightarrow w = \frac{2\pi}{\tau} \left( \frac{1}{4} + j \right)$	$\Leftrightarrow$	$\frac{w}{w_c} = \left( \frac{1}{4} + j \right)$	
$max \rightarrow w = \frac{2\pi}{\tau} \left( \frac{3}{4} + j \right)$	$\Leftrightarrow$	$\frac{w}{w_c} = \left( \frac{3}{4} + j \right)$	
$hifp \rightarrow w = \frac{2\pi}{\tau} \left( j + \frac{1}{2} \right)$	$\Leftrightarrow$	$\frac{w}{w_c} = \left( j + \frac{1}{2} \right)$	
$ifp \rightarrow w = \frac{2\pi}{\tau} j$	$\Leftrightarrow$	$\frac{w}{w_c} = j$	

(2)

and thus,  $\tau = \frac{2\pi}{w_c} = T_c$ . This interesting result confirms our previous approach about the physical insight of the

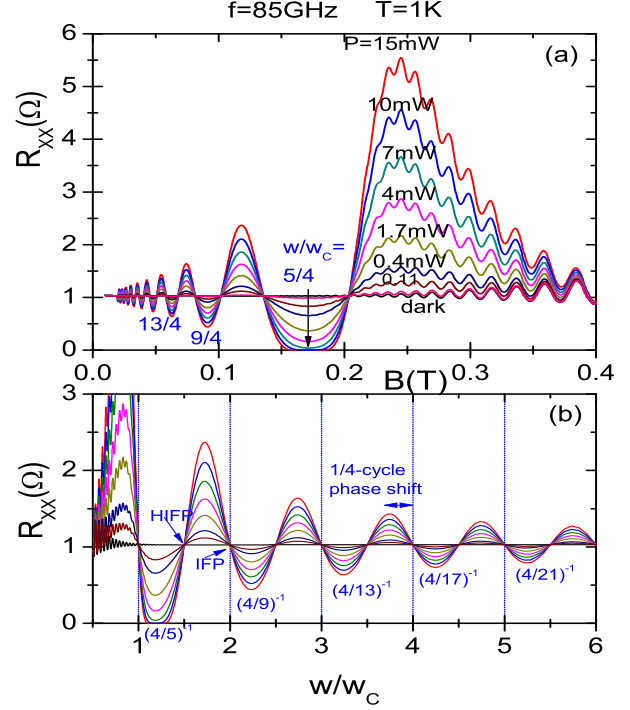


Fig. 2: Dependence of the extrema and nodes positions of MIRO with the radiation power. 2a) Calculated magnetoresistance,  $R_{xx}$ , irradiated with MW of 85 GHz vs  $B$  for different values of  $P$ , from 15 mW to dark and  $T = 1$  K. We observe how magnetoresistance oscillations tend to vanish as the power decreases. 2b) Same results as in 2a but this time vs  $w/w_c$ . In both panels we mark the values defining the  $1/4$ -cycle phase shift. The main result is that the positions of extrema and nodes are immune with respect to the power.

flight time. Now, the  $1/4$ -cycle phase shift of the MIRO minima can be traced back to a phase constant of  $\frac{\pi}{2}$  that is the delay that presents the driven guiding center with respect to radiation in the whole range of  $B$ . This delay is revealed by the interplay between the swinging nature of the Landau states under radiation and the remote charged impurity scattering. Then, we can state that the  $1/4$ -cycle phase shift in MIRO minima is an evidence of that the Landau states are not fixed but they oscillate driven by MW. The final expression of the irradiated magnetoresistance turns out to be:

$$R_{xx} \propto -\frac{eE_o}{m^* \sqrt{(w_c^2 - w^2)^2 + \gamma^4}} \sin \left( 2\pi \frac{w}{w_c} \right) \quad (3)$$

**Results..** – In Fig.1 we exhibit the dependence of MIRO extrema and nodes with respect to  $w$ . In Fig.1a, we show calculated irradiated  $R_{xx}$  versus  $B$  for an intermediate range of  $w$ . We observe, as expected according to the set of equations (3), that extrema and nodes displace to higher  $B$  as  $w$  increases. In Fig. 1b, we plot  $w_c$  vs  $w = 2\pi f$ , where  $f$  is the radiation frequency in GHz, for

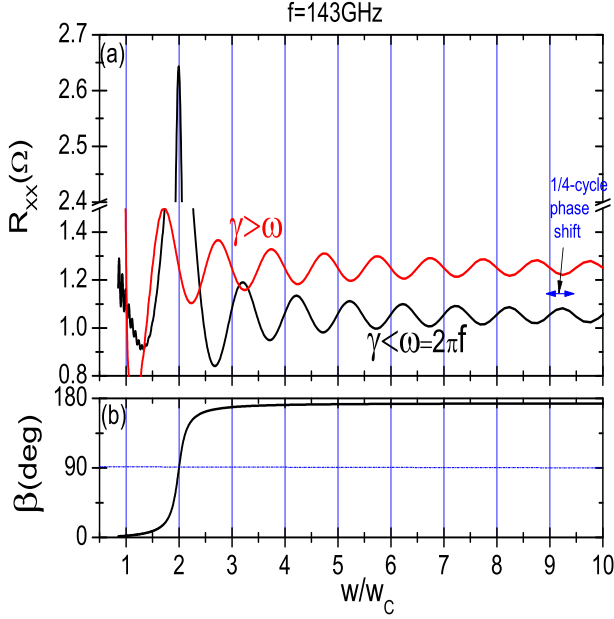


Fig. 3: Calculated magnetoresistance calculated results of irradiated  $R_{xx}$  and  $\beta$  vs  $w/w_c$  for a regime of  $\gamma < w$  and a frequency of 143 GHz. As in Y. Dai experiments, this simulations has been run considering that the resonance takes place in the second harmonic, i.e.,  $2w_c = w$ . This permits in the simulation to see more clearly the transition of  $\beta$  from  $\pi$  to  $\frac{\pi}{2}$ .

the extrema and nodes labelled in Fig. 1a. For the hifp we have used the square symbol, the index  $j = 1$  and then from equation (3) we obtain,  $w_c = w \times \frac{4}{6}$ . For the maxima, the black dot symbol, the index  $j = 1$  and then  $w_c = w \times \frac{4}{5}$ . For the ipf, the triangle symbol,  $j = 2$  and  $w_c = w \times \frac{4}{8}$ . And finally, for the minima, black down triangle,  $j = 2$  and  $w_c = w \times \frac{4}{9}$ . These calculated results demonstrate and explain that the corresponding shifts for extrema and nodes are independent of radiation frequency. They only depend on the phase difference between radiation and the harmonic displacement of the Landau orbit guiding center. In the lower panel we present the fits corresponding to the four set of data resulting, as expected, straight lines where the slopes are according to the extrema and nodes positions in the upper panel.

In Fig. 2, we present the  $P$  dependence of the extrema and nodes positions of MIRO. In Fig. 2a we plot  $R_{xx}$  irradiated with MW of 85 GHz vs  $B$  for different values of  $P$ , from 15 mW to dark and  $T = 1$  K. We observe how MIRO decrease and tend to vanish as  $P$  drops. In Fig. 2b, we exhibit same results as in 2a but this time vs  $w/w_c$ . In both panels we mark the values defining the 1/4-cycle phase shift. The main finding is that the positions of extrema and nodes turn out to be immune with respect to  $P$ . Now, we can theoretically explain these results according to our model. In equation (3)  $P$  only shows up in the numerator of the amplitude as  $\sqrt{P} \propto E_0$ , and not in the

phase of the sine function. Thus,  $P$  does not affect the phase of MIRO and the latter keeps constant. The outcome is that extrema and node positions in MIRO turn out to be immune to  $P$ .

Finally it is interesting to consider the case when the damping parameter  $\gamma$  is small compared to  $w$ . Under this condition we will come across with regimes where the 1/4-cycle phase shift will not be conserved. This can be found in ultra-high mobility samples where the damping parameter is expected to get smaller due to a much smaller disorder. Thus,  $\gamma < w \Rightarrow \gamma^2 \ll w^2$ , then the obtained values for  $\beta$  will be different from before when ramping up  $B$ . Thus, if along with this condition,  $w_c \simeq 0$ , (low values of  $B$ ), then  $\tan \beta \rightarrow 0$  and  $\beta \rightarrow \pi \Rightarrow X(t) = X_0 - A \cos(\omega t - \pi)$ . And we need to add an initial phase constant of  $-\frac{\pi}{2}$  to fulfill  $X(t = 0) = X_0$ . Finally  $X(t) = X_0 - A \cos(\omega t - \frac{3\pi}{2}) = X_0 + A \sin \omega t$ . Similarly as before, this result leads to  $\Delta X(t) = \Delta X_0 + A \sin \omega \tau$ . According to this we would expect different positions for extrema and nodes. For instance, now for maxima:  $\omega \tau = \frac{\pi}{2} + 2\pi j \Rightarrow w = \frac{2\pi}{\tau} (\frac{1}{4} + j)$ . And for minima:  $\omega \tau = \frac{3\pi}{2} + 2\pi j \Rightarrow w = \frac{2\pi}{\tau} (\frac{3}{4} + j)$ . These are opposite results to the ones obtained in the previous scenario of  $\gamma > w$ . If now  $B$  and  $w_c$  are increased,  $\tan \beta$  increases too, but in negative and tends to  $-\infty$  at resonance, where  $\beta \simeq \frac{\pi}{2}$ . Accordingly,  $X(t) = X_0 - A \cos(\omega t - \frac{\pi}{2} - \frac{\pi}{2}) = X_0 + A \cos \omega t$ , and now maxima positions are given by,  $\omega \tau = 2\pi j$ . If  $w_c$  keeps increasing,  $\tan \beta \rightarrow 0$  but now  $\beta \rightarrow 0$ . Thus, as  $B$  is ramping up from  $B = 0$ ,  $\beta$  evolves from  $\pi$  to  $\frac{\pi}{2}$  at resonance and, for higher  $B$ , ends up being equal to 0. Something similar to the above has been experimentally obtained previously by Y. Dai et al. [55] but it has been overlooked by the people, experimentalist and theorist, devoted to MIRO; they obtain a clear shift of extrema and nodes positions as  $B$  rises for ultra-high mobility samples.

In Fig. 3 we present calculated results of irradiated  $R_{xx}$  and  $\beta$  vs  $w/w_c$  for a regime of  $\gamma < w$  and a frequency of 143 GHz. As in Y. Dai experiments, this simulations has been run considering that the resonance takes place in the second harmonic, i.e.,  $2w_c = w$ . This permits in the simulation to see more clearly the transition of  $\beta$  from  $\pi$  to  $\frac{\pi}{2}$ . In the upper panel we plot two curves, one for  $\gamma < w$  (black curve) and the other for  $\gamma > w$  (red curve) to compare both regimes in terms of extrema and nodes positions as  $B$  rises. We observe that the black curve does not longer shows the 1/4-cycle phase shift for minima. Yet it presents this shift but for the maxima and changes to  $w = w_c j$  when approaching to  $w = 2w_c$ . In the lower panel it can be observed that the transitions persists up to  $\beta \simeq 0$  as  $B$  keeps increasing.

**Conclusions.** — In summary, we have presented a theoretical analysis of one of the main features of MIRO as is the 1/4-cycle phase shift of minima. We have used the radiation driven electron orbits model introducing the concept of flight time between Landau state in a scattering process. The first finding is that this time is equal to the



cyclotron period. We have obtained an exact coincidence between the calculated values for extrema and node positions and the experimental ones. The key outcome of our analysis is that this shift is an evidence of a delay of  $\frac{\pi}{2}$  between the oscillating Landau state guiding center and radiation. In consequence, the Landau states oscillates harmonically when irradiated and it is the interplay of this effect with scattering by charged remote impurities that gives rise of the appearance of MIRO. We have studied also the conditions so that this minima shift can be altered in ultra-high mobility samples.

**Acknowledgments.** — This work is supported by the MINECO (Spain) under grant MAT2014-58241-P and ITN Grant 234970 (EU). GRUPO DE MATEMATICAS APLICADAS A LA MATERIA CONDENSADA, (UC3M), Unidad Asociada al CSIC.

## REFERENCES

- [1] R. G. Mani, J. H. Smet, K. von Klitzing, V. Narayana-murti, W. B. Johnson, and V. Umansky, *Nature*(London) **420**, 646 (2002)
- [2] M. A. Zudov, R. R. Du, L. N. Pfeiffer, and K. W. West, *Phys. Rev. Lett.* **90**, 046807 (2003)
- [3] J. Iñarrea, G. Platero, *Phys. Rev. B*, **51**, 5244, (1995)
- [4] J. Iñarrea, R. Aguado, G. Platero, *Europhys Lett.* **40**, 417, (1997)
- [5] J. Iñarrea, G. Platero, *Europhys. Lett.*, **34**, 43, (1996)
- [6] A. N. Ramanayaka, R. G. Mani, J. Inarrea, and W. Wegscheider, *Phys. Rev. B*, **85**, 205315, (2012)
- [7] R. G. Mani, V. Narayanamurti, K. von Klitzing, J. H. Smet, W. B. Johnson, and V. Umansky, *Phys. Rev. B*, **69**, 161306(R), (2004)
- [8] R. G. Mani, J. H. Smet, K. von Klitzing, V. Narayana-murti, W. B. Johnson, and V. Umansky, *Phys. Rev. Lett.* **92**, 146801 (2004).
- [9] R. G. Mani, J. H. Smet, K. von Klitzing, V. Narayana-murti, W. B. Johnson, and V. Umansky, *Phys. Rev. B* **69**, 193304 (2004).
- [10] R. L. Willett, L. N. Pfeiffer, and K. W. West, *Phys. Rev. Lett.* **93**, 026604 (2004).
- [11] R. G. Mani, *Physica E (Amsterdam)* **22**, 1 (2004);
- [12] J. H. Smet, B. Gorshunov, C. Jiang, L. Pfeiffer, K. West, V. Umansky, M. Dressel, R. Meisels, F. Kuchar, and K. von Klitzing, *Phys. Rev. Lett.* **95**, 118604 (2005).
- [13] Z. Q. Yuan, C. L. Yang, R. R. Du, L. N. Pfeiffer and K. W. West, *Phys. Rev. B* **74**, 075313 (2006).
- [14] Tianyu Ye, Han-Chun Liu, Zhuo Wang, W. Wegscheider and Ramesh G. Mani, *Sci. Rep.* **5**, 14880, (2015)
- [15] R. G. Mani, and A. Kriisa, *Sci. Rep.* **3**, 3478, (2013)
- [16] R. G. Mani, *Appl. Phys. Lett.* **85**, 4962, (2004)
- [17] R. G. Mani, W. B. Johnson, V. Umansky, V. Narayana-murti and K. Ploog, *Phys. Rev. B* **79**, 205320 (2009).
- [18] S. Wiedmann, G. M. Gusev, O. E. Raichev, A. K. Bakarov, and J. C. Portal, *Phys. Rev. Lett.*, **105**, 026804, (2010)
- [19] S. Wiedmann, G. M. Gusev, O. E. Raichev, A. K. Bakarov, and J. C. Portal, *Phys. Rev. B*, **81**, 085311, (2010)
- [20] D. Konstantinov and K. Kono, *Phys. Rev. Lett.* **103**, 266808 (2009)
- [21] S. I. Dorozhkin, L. Pfeiffer, K. West, K. von Klitzing, J. H. Smet, *Nature Physics*, **7**, 336-341, (2011)
- [22] R. G. Mani, C. Gerl, S. Schmult, W. Wegscheider and V. Umansky, *Phys. Rev. B* **81**, 125320, (2010)
- [23] R. G. Mani, A. N. Ramanayaka and W. Wegscheider, *Phys. Rev. B*, **84**, 085308, (2011)
- [24] Jesus Inarrea, R. G. Mani and W. Wegscheider, *Phys. Rev.* **82** 205321 (2010)
- [25] R. G. Mani, *Int. J. Mod. Phys. B*, **18**, 3473, (2004); *Physica E*, **25**, 189 (2004)
- [26] J. Iñarrea and G. Platero, *Phys. Rev. Lett.* **94** 016806, (2005)
- [27] J. Iñarrea and G. Platero, *Phys. Rev. B* **72** 193414 (2005)
- [28] J. Iñarrea and G. Platero, *Appl. Phys. Lett.*, **89**, 052109, (2006)
- [29] J. Iñarrea and G. Platero, *Phys. Rev. B*, **76**, 073311, (2007)
- [30] J. Iñarrea, *Appl. Phys. Lett.* **90**, 172118, (2007)
- [31] A. C. Durst, S. Sachdev, N. Read, S. M. Girvin, *Phys. Rev. Lett.* **91** 086803 (2003)
- [32] X. L. Lei, S. Y. Liu, *Phys. Rev. Lett.* **91**, 226805 (2003)
- [33] Ryzhii et al, *Sov. Phys. Semicond.* **20**, 1299, (1986)
- [34] P. H. Rivera and P. A. Schulz, *Phys. Rev. B* **70** 075314 (2004)
- [35] M. G. Vavilov et. al., *Phys. Rev. B*, **70**, 161306 (2004)
- [36] J. Iñarrea and G. Platero, *Appl. Phys. Lett.* **93**, 062104, (2008)
- [37] J. Iñarrea and G. Platero, *Phys. Rev. B*, **78**, 193310, (2008)
- [38] J. Iñarrea, *Appl. Phys. Lett.* **92**, 192113, (2008)
- [39] Jesus Inarrea and Gloria Platero, *Appl. Phys. Lett.* **95**, 162106, (2009)
- [40] J. Iñarrea, *Appl. Phys. Lett.* **90**, 262101, (2007)
- [41] J. Inarrea, G. Platero and A. H. MacDonald, *Physica Stat. Solid. A*, **203**, 1148, (2006)
- [42] J. Iñarrea, *Appl. Phys. Lett.* **100**, 242103, (2012)
- [43] Tianyu Ye, Han-Chun Liu, W. Wegscheider and R. G. Mani, *Phys. Rev. B*, **89**, 155307, (2014)
- [44] Q. Shi, P. D. Martin, A. T. Hatke, M. A. Zudov, J. D. Watson, G. C. Gardner, M. J. Manfra, L. N. Pfeiffer and K. W. West, *Phys. Rev. B*, **92**, 081405(R), (2015)
- [45] M. A. Zudov, *Phys. Rev. B*, **69**, 041304(R), (2004)
- [46] J. Inarrea and G. Platero, *Appl. Phys. Lett.* **89**, 172114, (2006)
- [47] E. H. Kerner, *Can. J. Phys.* **36**, 371 (1958).
- [48] K. Park, *Phys. Rev. B* **69** 201301(R) (2004).
- [49] A. P. French, *Vibrations and waves.*, W. W. Norton and Company, New York, 1971.
- [50] I. G. Main, *Vibrations and waves in Physics.*, Cambridge University Press, 1993.
- [51] Noboru Miura, *Physics of Semiconductors in High Magnetic Fields.*, Oxford University Press, (2008).
- [52] Jesus Inarrea and Gloria Platero, *Journal of physics. Condensed matter* **27** 415801 (2015)
- [53] Claude Cohen-Tannoudji, Bernard Diu and Franck Laloe, *Quantum Mechanics*, John Wiley and sons, New York, (1977).
- [54] B. K. Ridley. *Quantum Processes in Semiconductors*, 4th ed. Oxford University Press, (1993).
- [55] Yanhua Dai, R. R. Du, L. N. Pfeiffer and K. W. West, *Phys. Rev. Lett.* **105** 246802 (2010)